Laser Doppler Anemometry Investigation on Sub Boundary Layer Vortex Generators for flow control

J G Betterton, K C Hackett, P R Ashill, M J Wilson, I J Woodcock
JBetterton@DERA.gov.uk
DERA Bedford, UK

C P Tilman, K J Langan
Carl.Tilman@va.afrl.af.mil
Air force Research Laboratory, USA

Abstract

A three component Laser Doppler Anemometry (LDA) system has been used as the primary measurement instrument for a programme of work investigating the fundamental behaviour of sub boundary layer vortex generators. Report on the effect of SBVG on three common flows of interest; a zero pressure gradient, an equilibrium pressure gradient and a 2D turbulent boundary layer flow separation. Four Generic designs of passive vortex generator have been studied and one active design using pulsed air jets[2].

Studies have been performed in the DERA Bedford Boundary Layer Tunnel. The tunnel is of open return design with a long working section 1.2m wide by a nominal 0.3m high. The tunnel floor is flexible and the growth of boundary layers along the working section can be controlled by the developed local pressure gradient[1]. More highly complex flows can be achieved by additionally fixing flow-forming structures within the working section. The LDA system used two TSI fibre optic coupled probe units fitted with beam expansion optics and 205mm diameter, 1540mm focal length lenses. Probes were configured as a symmetric system with a subtended half angle of 20.1° and mounted on a 0.6m motion three-axis traverse. Data collection utilised Dantec enhanced BSA processors and software.

Results presented characterise downstream circulation, vortex position, trajectory and persistence with methods of SBVG classification by non-dimensional parameters. The effect of pressure gradient on downstream flow is demonstrated. It is shown that SBVG devices with heights in the order of only one quarter of the boundary layer can significantly reduce the size of regions containing turbulent boundary layer separated flow.

1. Introduction

Improvements in cruise and manoeuvre performance of both military combat and civil transport aircraft can only be achieved through a better understanding of flows over their lifting surfaces. At manoeuvre conditions aircraft need to generate high lift coefficients to achieve the desired performance. This is either because only a component of the lift is available to counter the aircraft weight, as in turning manoeuvres, or because the aircraft speed has to be low, as in landing and take-off. Most of this lift is generated on the wing upper surface, where the pressures are generally lower than at the wing trailing edge. Therefore there can be large positive pressure gradients on the wing. A possible consequence is that the boundary layer separates, causing, in turn, a loss of lift, high drag and buffeting.

At low speed the flow separations can either occur near the wing leading or trailing edges, depending on the wing geometry and the angle of incidence of the wing. In high-speed manoeuvres they may occur downstream of shock waves, causing bubbles that may burst or join up with trailing-edge separations to cause flow breakdown.

The problem of designing wings to achieve high lift coefficients without flow separation has occupied aerodynamicists for many years. During this time techniques have been developed to prevent or delay flow separation. These techniques include: slotted flaps (both at the leading and trailing edges), blowing, suction and Vortex Generators (VGs). The last of these techniques has been used to control flow separation on a number of aircraft in recent years. The attraction or otherwise of these devices depends on their effect on the aircraft performance over the whole flight envelope. Thus it is sometimes argued that the use of VGs should be avoided since they incur a drag penalty in parts of the flight envelope other than those for which they have expressly been designed, for example during the cruise.

Criticisms of VGs are usually based on a purely aerodynamic view of the problem and ignore the possible multi-disciplinary benefits of VGs such as the opportunity to have wings of greater thickness or higher taper. This would lead to wings of lower weight and larger fuel volume. Furthermore, the argument against VGs would carry less force if they could be designed to have low parasitic drag. This has led researchers to investigate Sub Boundary layer VGs (SBVGs). Being small and buried within the relatively-low energy flow within the boundary layer, these devices may be expected to have low drag, while perhaps inducing vortices of sufficient strength to induce the mixing in the boundary layer needed to control separated flows.

Vortex generators have also been used to enhance the lift obtained from slotted flaps[4]. For this purpose, the parasitic drag of the vortex generators is a less important issue than the additional lift provided because the devices are stowed within the wing during cruise. However, they still need to be small enough for the available space within the wing, and, if their parasitic drag were sufficiently large, they might adversely affect climb performance. Thus the study of SBVGs is justified for this application as well.

Another attraction of miniature vortex generators is that the power needed to drive them for active control (e.g. as 'pop-up' devices) is relatively low and so they might be used as part of an active system over a wide range of flow conditions. In this role they could be part of a system using Micro Electro-Mechanical Systems (MEMS) as motivators and sensors. As well as controlling flow separation they could be used for direct-lift control or lateral control.

Furthermore, the use of jets of air emerging at an angle from the wing surface to produce a similar type of vortex flow to traditional VGs are also being investigated[2]. The air jet vortex generators (JVG) can be steady with time or pulsed in operation (PJVG) and offer active type flow control without the need of a protruding physical device on the wing surface.

This paper reports on work performed in the second year of an experimental investigation on the flow downstream of SBVGs and PJVGs which has been in association with a TTCP collaboration with the Air force Research Laboratory, USA. The work was performed to gain an understanding of the physical processes involved in the production of the vortices and their interaction with one another, the surrounding boundary layer upstream and downstream of separation. Investigation of VG geometry in order to determine the most efficient arrangement in terms of effectiveness in reducing the extent of flow separation with minimum increase in drag.

Further work to assess the accuracy of CFD methods for predicting the flows around sub boundary-layer devices, their effect on separated flows and to provide correlation algorithms that might be used for the design of suitable devices for controlling flow separation will be reported[3].

2. Experimental techniques

Use has been made of the DERA Boundary Layer Tunnel facility with a three-component Laser Doppler Anemometer (LDA) to perform detailed flow measurements downstream of a number of different types of SBVG and PJVG. These measurements have been made in three types of flow with a turbulent boundary layer, representing differing degrees of severity imposed on the flow induced by the SBVGs.

2.1 Laser Doppler Anemometry

The three-component LDA system used for these measurements can be described as a commercial hybrid. Coherent light was provided by a standard Spectra Physics 165 CW Argon-Ion laser operating TEM_{00} at 4.0W multiline and coupled into a TSI colorburst, hence through optic fibre transmission to a pair of TSI back-scatter probe units enabling three-component velocity data collection. Beam expansion extensions were used to utilise 205mm diameter back-scatter collection lenses at 1540mm focal length. Burst processing was performed by three Dantec Enhanced BSA processors and Burstware 3.21 software running over a local PC network. Probes were configured as a symmetric system with a subtended half-angle of 20.1°. Traversing the LDA measurement volume over the region of interest was handled by a lightweight Techno-Isel 0.6m range XYZ traverse under automated Dantec software control. The combination of products was found to be very effective for data collection.
At each data station approximately 10,000 validated Doppler bursts were processed by each of the three BSA units before being used for calculation of resolved orthogonal u,v,w velocity vectors.

Figure 1 Laser Doppler Anemometry measurement in the DERA Bedford Boundary Layer Tunnel.

2.2 Boundary Layer Tunnel facility

The DERA Boundary Layer Tunnel used for this investigation (Fig 1) is of the open return type, and has a closed test section. The test section is 5.49m long, 1.2m wide and has a flexible floor allowing the streamwise pressure distribution in the working section to be adjusted. A maximum test section height of 0.7m can be achieved, the standard height being 0.3m. An important feature of this wind tunnel is the facility to set up boundary-layer flows with various streamwise pressure distributions at reasonably large aerodynamic scale. For most of the work to be described in this report the floor was set to give a flow with nominally zero pressure gradient along the roof, the flow illustrated in Fig 1a. In addition, the shape of the floor was adjusted to achieve the pressure distribution calculated to give an equilibrium boundary layer in the absence of any devices (Fig 1b). Finally, a bump was mounted on the roof to simulate the flow illustrated in Fig 1c. The SBVGs were either mounted on the roof of the test section or on the bump.

2.3 Flows studied

Three types of basic flow have been studied, which are representative of those found on aircraft wings. These are illustrated on the left-hand side of Fig 2 alongside the equivalent simulations of the upper-surface pressure distributions established on the roof of the test section of the DERA Boundary-layer Wind Tunnel and the representative tunnel working section profile. The measured pressure distributions are defined by the pressure coefficient Cp*, which is derived by reference to the flow conditions at the most downstream measurement station in the tunnel. This definition is used so that the pressure distributions resemble those measured on a wing in free air. The first flow considered has essentially zero pressure gradient, representing a flat ‘rooftop’ region upstream of a shock wave (Fig 2a). It also provides a datum case, to aid the understanding of the flow downstream of the SBVGs without the complication of pressure-gradient effects. The aerodynamic effects of all the chosen SBVG devices were studied on this flow along with the active PJVGs.

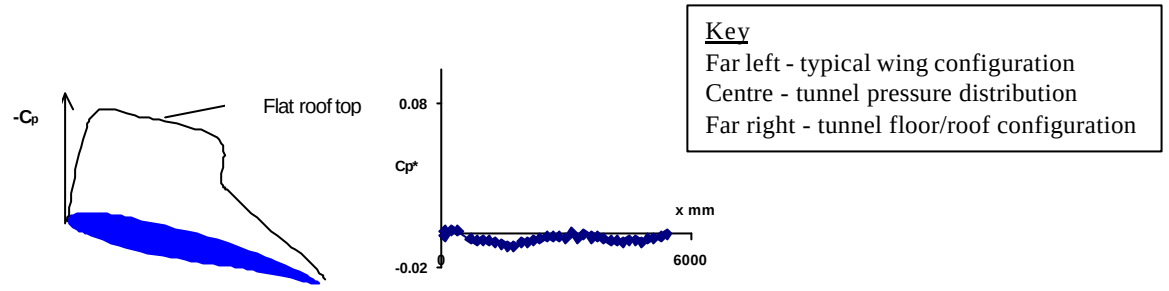

A) zero pressure gradient flow, i.e. transonic wing

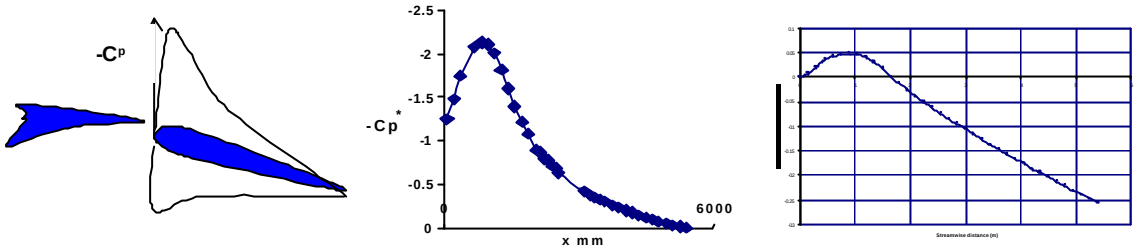

B) equilibrium adverse pressure gradient flow, i.e. high lift wing flap

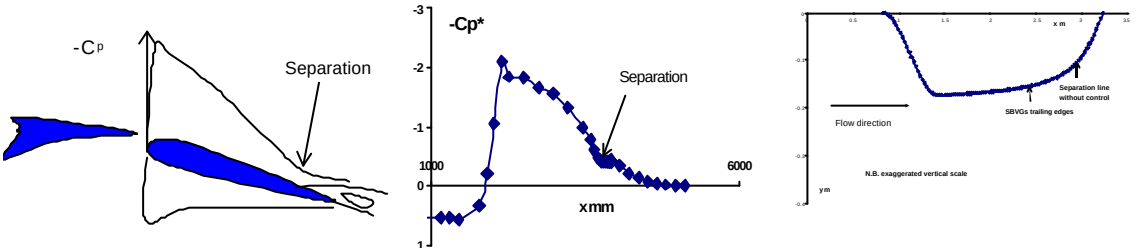

C) separating flow, i.e. stalling high lift wing flap

Figure 2 characteristic flows studied

The second flow has a pressure gradient which represents a case that has been calculated to have the largest adverse pressure gradient that can occur in turbulent boundary layers that are in equilibrium (i.e. with similar velocity profiles) at the Reynolds number of the test. In this case the boundary layer resembles that for an attached flow on the upper surface of a wing or a flap (Fig 2b). Over almost the whole length of the test section the distribution of the streamwise velocity just outside the boundary layer has the form,

$$U_e \propto (x - x_0)^{-m}$$

where x is streamwise distance, suffix 0 refers to a reference position and m is a positive index. In this region the boundary layer is said to be in equilibrium because the velocity and shear-stress profiles at different streamwise stations are similar[7]. The inward displacement of the floor of the test section to achieve this flow is illustrated.
The third case is an example of a flow well removed from equilibrium, where a rapid rise in pressure, downstream of a region of mild adverse pressure gradient, results in flow separation. The flow is representative of a range of separated flows on wings and flaps, as shown in Fig 2c and was achieved by installing a bump on the roof of the tunnel working section while keeping the floor straight. The bump was located such that its trailing edge was 3.23m downstream of the entrance to the working section and had a shape as described. The main requirement in setting up this flow was to ensure a reasonable extent of quasi two-dimensional flow at the intended position of the SBVGs. This proved difficult to achieve - a fact that was to be expected in view of the known sensitivity of separated flows to small disturbances. It was found necessary to ensure that leaks between the working section and outside were minimised by sealing before an acceptable flow could be obtained. After this had been done an acceptable flow with a region of quasi-2D flow occupying about 70% of the span of the bump was obtained.

2.4 Flow control devices

A number of different device shapes and heights have been studied and are summarised in Figure 3. With a maximum height of 30 mm these devices are large enough to allow detailed surveys to be made by the LDA in the region where the vortices are created. In addition, they are sufficiently large for the Reynolds number based on their height to be representative of that for SBVGs on aircraft wings. The devices studied include those creating counter-rotating vortices (wedges and counter-rotating vanes) and single rotation devices (vanes).
The coverage of parameters of the experiment with zero pressure-gradient was fairly comprehensive. However, the investigation with the equilibrium adverse pressure gradient has to date been restricted to the effects obtained with one configuration, the joined Counter-rotating vanes at a height of 30 mm.
The PJVG investigated was of a design specified by AFRL which has a 10mm diameter air tube inclined at 45° in the cross flow plane and perpendicular to the freestream. The jet pulse was solenoid actuated and regulated by a digital mass flow meter. The device was mounted into a tunnel insert so presented no physical intrusion into the flow.

3. Results and discussion

3.1 SBVGs in a zero pressure gradient.

For the zero pressure gradient flows each device was studied at nominal air speeds of 10, 20, 30 and 40m/s when measured at the tunnel throat, and at a fixed distance of 5 device heights (5h) downstream of the device trailing edge. At fixed speeds of 30m/s cross-flow planes were investigated at downstream distances 0.5 device heights (0.5h), 5h, 10h and 15h. Each device was tested in a 30mm height configuration and the forwards wedge was further tested in 15mm and 5mm height configurations.
The vortex strength at a particular streamwise station is found by calculating the circulation around a contour in the cross-flow plane surrounding a vortex core. This contour comprised a rectangle of sides 2.5h by 3h, the height of the centre of area of which was adjusted so that the core was roughly at the same height. Referencing the contour dimensions to a dimension of the device ensures a consistent scaled definition of circulation regardless of device height. For counter-rotating devices the circulation is defined as the arithmetic mean of the absolute values of the circulation of separate vortices on either side of the geometric plane of symmetry. For the single vortex device, the circulation is the absolute value of the measured circulation. Results from this method have been compared to those from various plane integration algorithms and were found to be favourable.
The difference between the absolute values of the circulation of each the vortex of the pair generated by the counter-rotating devices was found to be typically less than 10% in zero pressure gradient. However, larger differences were found in the equilibrium flow with an adverse pressure gradient.

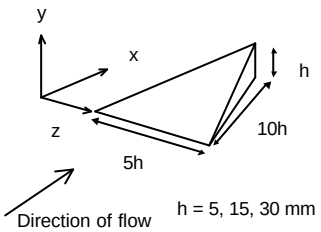

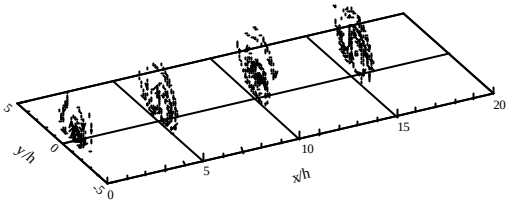

a) forwards wedge

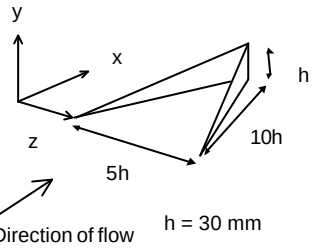

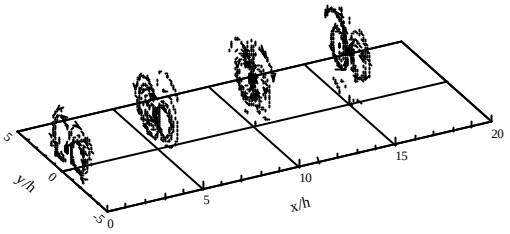

b) joined vanes

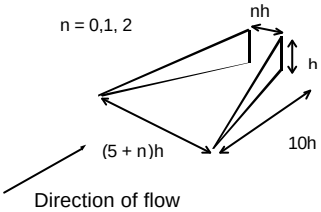

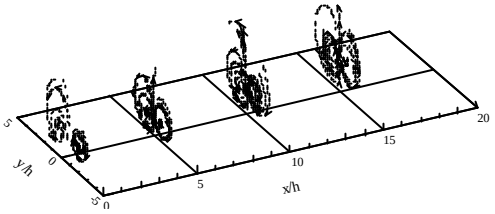

c) spaced counter rotating vanes

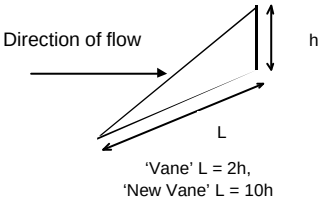

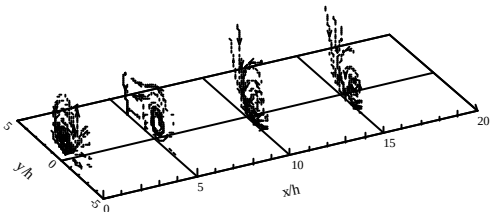

d) single vanes

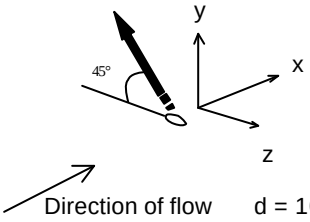

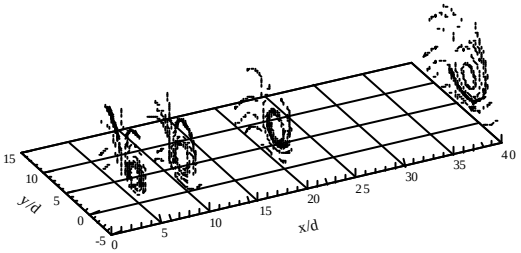

e) pulsed jets

Figure 3 Devices tested accompanied by downstream progressions of cross-flow steamlines showing typical vortex structure.

The main source of error in the determination of circulation is considered to be the variability of the tunnel speed during a traverse. Errors in circulation from this source are estimated to be within the range ±1% at a tunnel speed of 30 m/s, rising to ±3% at 10 m/s.
The position of the vortex core was defined as the centre of the region where the vorticity was concentrated. This was inferred from plots of vortex vectors in cross-flow planes, and the uncertainty of the estimate in both vertical and lateral positions is estimated to be less than 2% of device height.

3.2 Vortex strength for SBVGs

Consider a vortex generator placed within the 'inner region' of a turbulent boundary layer. Dynamic similarity of flows requires that the circulation, Γ, around one of the vortices at a particular streamwise station correlates with the height of the device and the wall friction velocity u_τ (in the absence of the device) in either of the following ways:

$$\frac{\Gamma}{u_t h} = f(h^+),$$

$$\frac{\Gamma}{n} = g(h^+).$$

Here

$$u_t = U_e \sqrt{C_f / 2},$$

Ue is the streamwise velocity at the outer edge of the boundary layer in the empty tunnel, Cf is local skin-friction coefficient of the undisturbed boundary layer and

$$h^+ = u_t h / n$$

is a device Reynolds number.
Using results derived from LDA measurements, Fig 4 shows plots of the non-dimensional circulation $\Gamma_5/u_\tau h$ against h+ for various types of SBVG. The suffix 5 denotes that the measurements are made at a distance of 5 device heights downstream of the device, $(x - x_t) = 5h$, and xt is the streamwise position of the trailing edge of the device. This figure shows that for values of h+ above between 750 and 2800 the non-dimensional circulation varies only slightly with h+. Experimental data at lower values of h+ are only available for the Forwards wedge and these show that the non-dimensional circulation decreases as h+ approaches zero. Here it should be noted that at the device location, the non-dimensional boundary-layer thicknesses, $u_\tau\delta^*/\nu$ and $u_\tau\delta/\nu$, of the undisturbed flow are approximately 600 and 4300, respectively, for a free-stream speed of 30 m/s, with slight variations over the range of wind speeds tested. This indicates that the variation of non-dimensional circulation with device height can reasonably be ignored for devices that are higher than the boundary-layer displacement thickness.

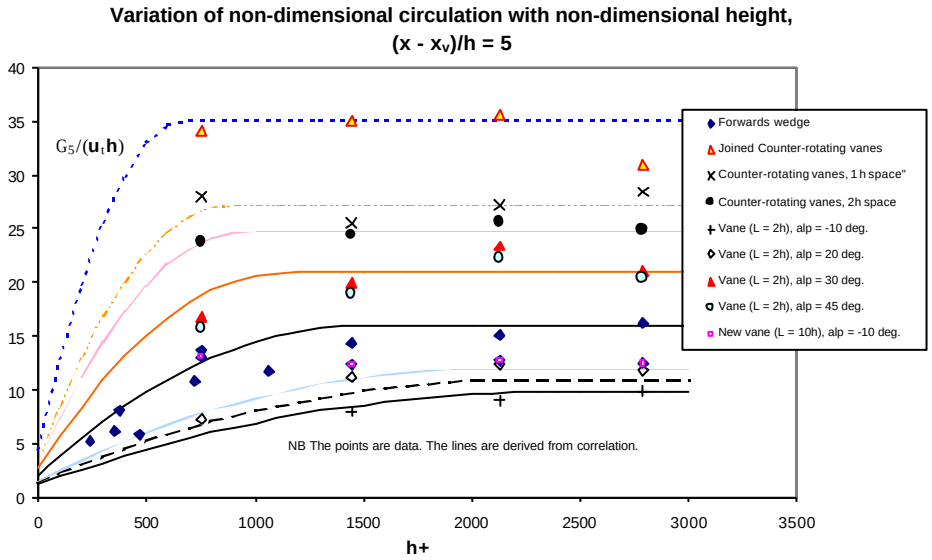

Figure 4 Non dimensional circulation versus non dimensional device height, zero pressure gradient

This shows that the maximum value of non-dimensional circulation $\Gamma_5/u_\tau h$ reached at high Reynolds number depends on the type of device, the largest value being obtained with the Joined vane. Again, this dependence on geometry is not surprising, and it does suggest a framework for generalising the correlation by using the concept of an effective height. For this purpose the effective height of the Forwards wedge is taken to be equal to its geometric height, or, in other words, the Forwards wedge is regarded as a datum. The effective heights of the other devices are then selected by ensuring that the maximum value of non-dimensional circulation based on this effective height is independent of device geometry. Table 1 displays a table of effective device heights. The effective height does not have a particular relationship to any physical dimension but is merely a convenient way of collapsing the data. A good correlation can be found between the collapsed data and a curve fit[3] providing a basis for predicting the vortex strength just downstream of SBVG devices for a wide range of device Reynolds numbers and a number of types of device.

Device	Effective device height h/he
Forward wedge	1.0 (datum)
Joined counter-rotating vanes	2.2
Counter-rotating vanes, 1h spacing	1.7
Counter-rotating vanes, 2h spacing	1.55
Vane (L=2h), alp = -10 deg	0.618
Vane (L=2h), alp = 20 deg	0.744
Vane (L=2h), alp = 30 deg	1.31
Vane (L=2h), alp = 40 deg	1.27
New Vane (L=10h), alp = -10 deg	0.79

Table 1 effective device heights

3.3 Vortex decay

To illustrate the decay of the (mean) vortex strengths for counter-rotating, Fig 5 shows a plot of $\ln(\Gamma/\Gamma_{0.5})$ against $(x - x_t)/h$ for devices with h = 30mm and for $U_e \approx 30$m/s ($h^+ \approx 2800$). Here suffix 0.5 denotes conditions (measured by LDA) at a distance of 0.5h downstream of the device (i.e. very close to the trailing edge of the device). The data are plotted in this form in view of the observation that circulation of well-spaced vortices decays in an exponential fashion with streamwise distance[4]. This shows clearly that the streamwise decay of vortex strength for the two spaced Counter-rotating vane configurations is much lower than for the Forwards wedge and the joined Counter-rotating vanes. For the Forwards wedge and the joined vane device this can be explained by the proximity of the counter-rotating vortices to one another. Owing to mutual interference between the two vortices, this results in a reduction in vortex strength. This is an important result, showing the potential benefit of having spaces between the counter-rotating vortices.

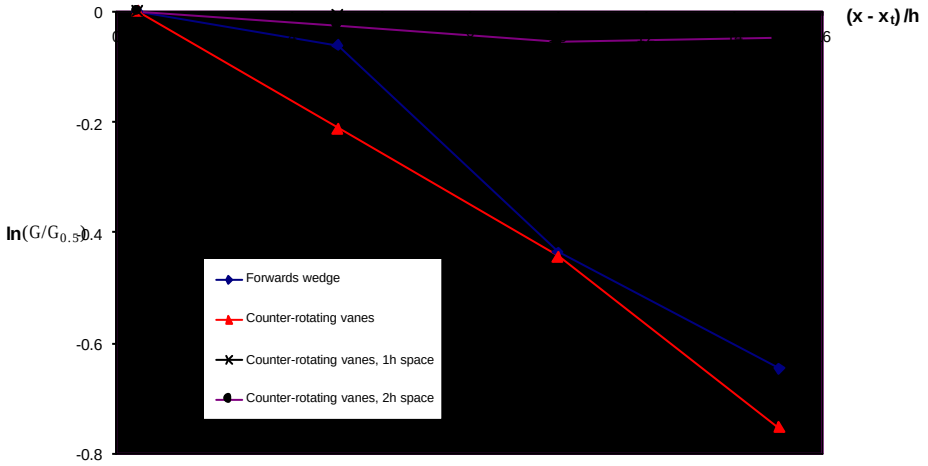

Figure 5 Decay of vortices downstream of various devices, zero pressure gradient, h = 30mm, U_e » 30m/s

3.4 Vortex trajectories

The vortex trajectory can play a crucial role in the performance of SBVGs. One of the primary objectives of a VG used in flow control is to mix highly energetic air from outside the boundary layer (BL) into the slower moving boundary layer region. This is achieved by positioning the vortex such that it straddles the edge of the BL in the downstream region of the flow at most risk of separation. Conventional Co-rotating VGs and PJVGs produce a vortex at the required height from the surface that does not significantly lift or fall in the trajectory downstream. SBVGs by their nature produce vortices deep within the BL and generally use a counter rotating vortex pair to enable interaction and a resultant trajectory that lifts away from the surface toward the BL edge.

Paths of the centres of the vortex cores inferred from the LDA measurements are shown in Figure 6 for three different types of counter-rotating SBVG. These include the Forwards wedge, the joined Counter-rotating vanes and the Counter-rotating vanes spaced apart by 1h, respectively. Each figure shows the trajectories of the two vortices in the cross-flow plane (y, z).

In the case of the Forwards wedge, the vortices move away from the wall and tend to move apart as they progress downstream. The path of the vortex at negative z is somewhat distorted, a result that is not easily understood but may be due to slight asymmetries either in the flow or in the model. Generally similar experimental form for the joined Counter-rotating vanes are indicated but with greater movement, probably resulting from the stronger vortices. Here excellent symmetry is observed between the vortex pair in the cross-flow plane. The vortices initially lift without separating before starting to move apart downstream of about $(x - x_t) = 5h$. Comparing the height of the vortex pair close to the trailing edge at $(x - x_t) = 0.5h$ is noticeably greater for the joined Counter-rotating vanes than for the Forwards wedge and that this bias remains with distance downstream.

The Counter-rotating vanes with 1h space at the apex provide a contrasting result. The vortices have a wider spread close to the trailing edge at 0.5h than for the other two devices. In addition, there is a significant inward movement together of the vortices to $(x - x_t) = 10h$. This inward movement is accompanied by only a modest vertical displacement up to $(x - x_t) = 5h$. The more rapid rise further downstream is not, however, accompanied by any separation of the vortices, at least within the $(x - x_t) = 15h$ limit of the experiment. At $(x - x_t) = 15h$ there is a greater vertical movement of the vortex at negative z but this displacement is not as great as that for the joined vanes.

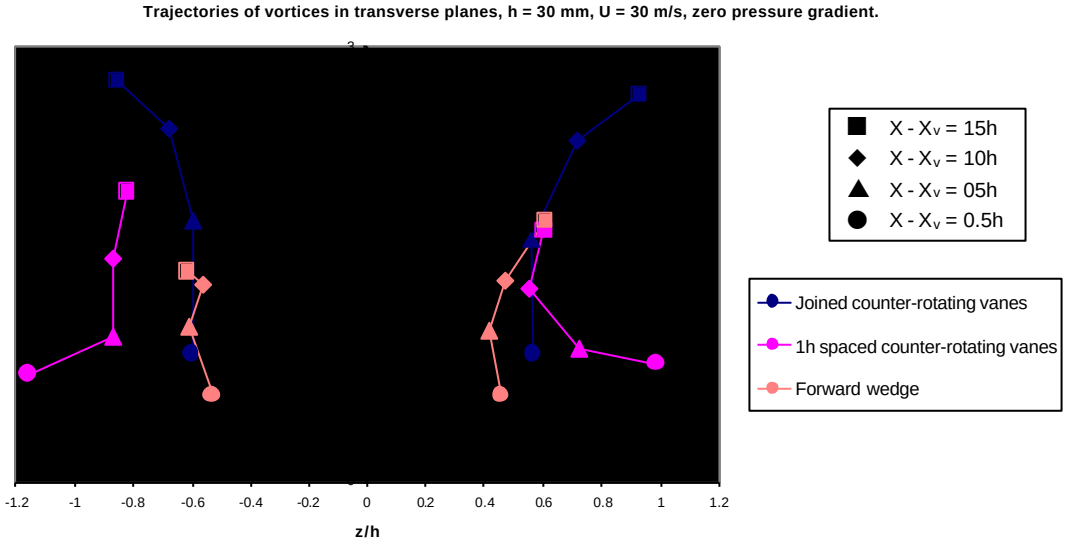

Figure 6 new vortex trajectory plot

4. Equilibrium adverse pressure gradient flows

The device was studied at nominal air speeds of 10, 20, 30 and 40m/s when measured at the tunnel throat, and at a fixed distance of 5 device heights (5h) downstream of the device trailing edge. At fixed speeds of 30m/s cross-flow planes were investigated at downstream distances 0.5 device heights (0.5h), 5h, 10h and 15h. The method of analysis used in the study of SBVGs in zero pressure gradient, has been extended to the investigation of the joined Counter-rotating vanes (h = 30 mm) in the equilibrium adverse pressure gradient flow at U_e = 30 m/s. The non-dimensional circulation $\Gamma_5/u_\tau h$ includes an allowance for differences in local streamwise velocity outside the boundary layer and the change in shape of the inner part of the boundary layer. Thus it might be expected that this parameter would be insensitive to pressure gradient. The table below shows a comparison between the values of non-dimensional circulation for the adverse pressure gradient and zero pressure gradient cases for U_e = 30 m/s.

Case	$G_5/u_t\,h$	h^+
Adverse pressure gradient	22.78	1287
Zero pressure gradent	35.65	2131

Table 2 Comparison of non-dimensional circulation in zero and adverse pressure gradients.

In fact, the value of non-dimensional circulation measured in the adverse pressure gradient is significantly lower than that for zero pressure gradient. This suggests that the effective height of the device is reduced by the adverse pressure gradient. Noting that the effective height of the joined Counter-rotating vanes in zero pressure gradient he = 2.2h it may be inferred from the table above that the effective height in adverse pressure gradient he = (2.2x22.78/35.65)h = 1.41h. This neglects the effect of the change in the value of Reynolds number from the one case to the other but the values of h+ are sufficiently high for Reynolds-number effects to be ignored. The reasons for the effective height of the joined Counter-rotating vanes being lower in adverse pressure gradient than in zero pressure gradient are not known. However, it is possible that the device itself caused the boundary layer upstream of it to separate.

Figure 7 shows a comparison of the streamwise decay of vortex strength and cross-flow vortex paths measured in zero and adverse pressure gradients for the joined Counter-rotating vanes. Interestingly and somewhat surprising, the vortex decay in the adverse pressure gradient is similar to that for zero pressure gradient while the effect on streamwise velocity U is markedly different.

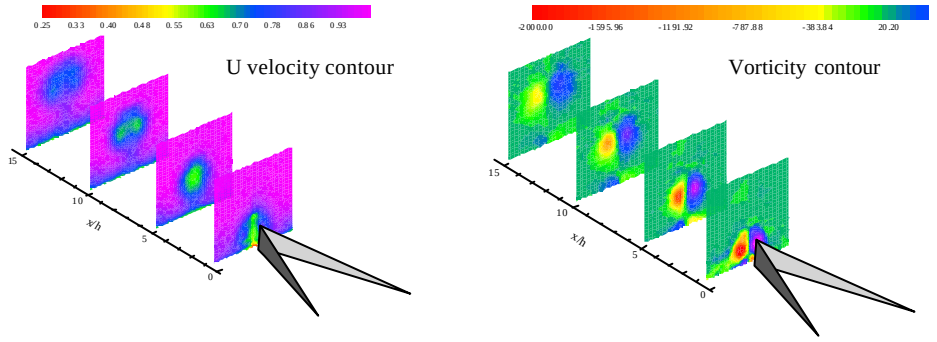

a) zero pressure gradient

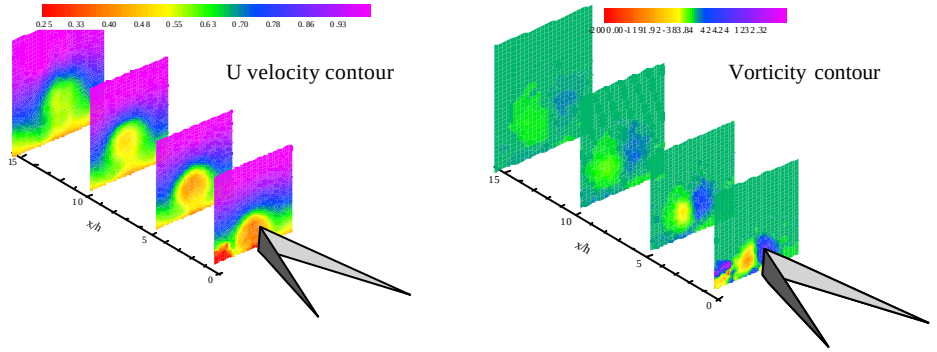

b) equilibrium adverse pressure gradient

Figure 7 Downstream contours of U velocity and vorticity for the joined counter-rotating vanes in a) zero pressure gradient and b) equilibrium adverse pressure gradient.

5. Pulsed Jet Vortex Generators in zero pressure gradient

As similar regime of testing was performed for the active PJVG where control variables of pulse duration, pulse frequency and jet velocity ratio were studied (Carl). PJVG data was collected in the zero pressure gradient flow at a fixed nominal tunnel speed of 30m/s. Pulse frequencies of 7.5, 15 and 30 Hz were investigated at velocity ratios (U_{jet}/U_{∞}) of 1.38, 1.84, 2,76 and 4.60. Duty cycle was also varied at 15, 25, 50 and 100%. This paper will overview this work and details are reported[2]. PJVGs offer an alternative to SBVGs as they are naturally a fully active device that can be engaged and disengaged very readily, there is also no physical object intruding into the flow during operation.

Pulsing jets can be seen to be as effective at producing vortical flow as steady jets with using lower mass flows of air, however the mechanics behind the formation of the vortex is less well understood. This study has concentrated on device configurations suitable for use in arrays co-rotating VGs in that the vortex core is developed near the edge of the boundary layer and experiences only a small variation of height from the surface as it progresses downstream. Figure 8 displays a typical effect on the vortex position with jet velocity ratio.

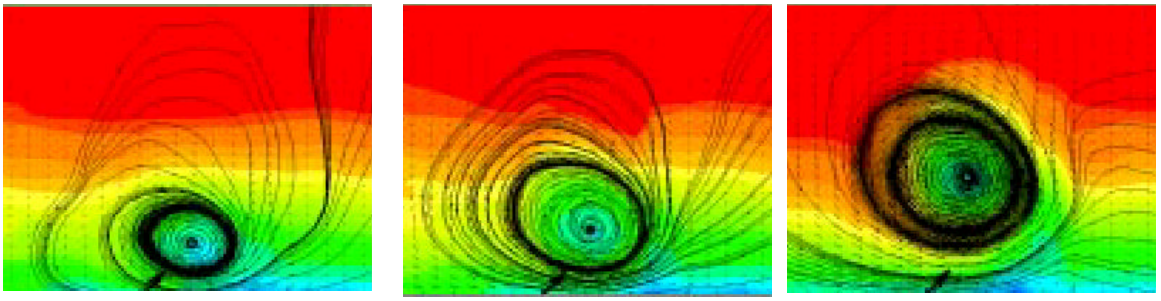

a)Velocity Ratio = 1.5 b) Velocity Ratio = 2.0 c) Velocity ratio = 2.94

Figure 8 Typical effect on the position of the primary vortex with jet velocity ratio ($U_{jet}/U_{¥}$) at 20 jet diameters downstream. Contours of U velocity and secondary streamlines of v,w.

6. Control of separation (bump flows)

Flow control devices tested on the separating flow were modelled in arrays of 8 devices spaced at 12 device heights apart and covered the full tunnel width. Tested were forward wedges, joined counter-rotating vanes and counter-rotating vanes that had an open space of 1 device height or 1h at the apex. All were of height h = 10 mm which was approximately 0.25 of the boundary layer thickness over the device. The separating flow was studied at a tunnel condition of 20m/s at the throat which resulted in a nominal 40m/s air flow through the additional 'bump' contraction and at the point of flow separation.

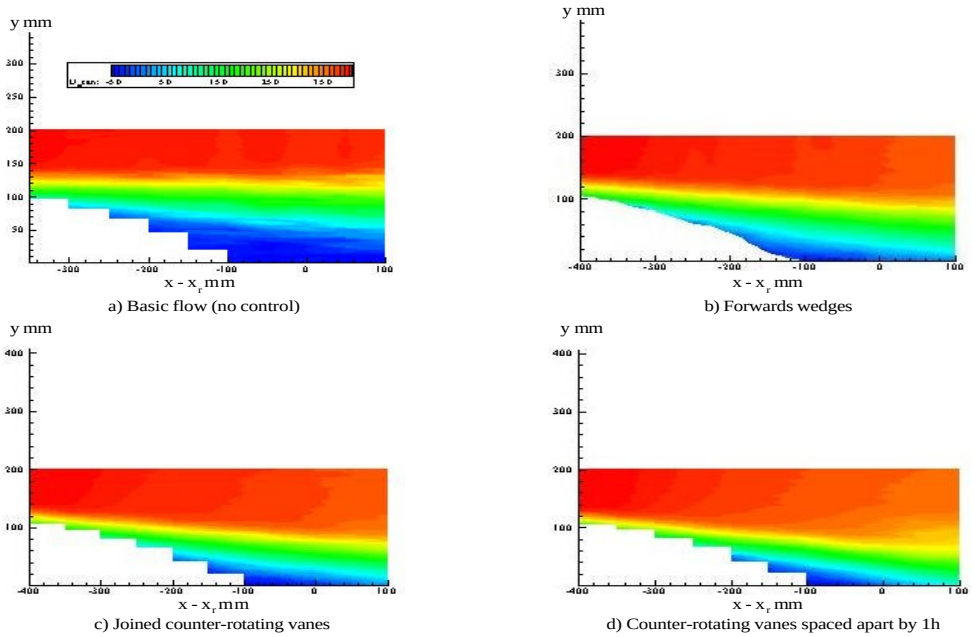

Figure 9 Contours of constant streamwise velocity in a vertical plane of symmetry over the separated flow.

Figure 9 shows results for velocity distributions at the vertical plane of symmetry 'above' the bump, where different colours indicate contours of constant velocity. The pictures in these figures illustrate the flow over the rear of the bump with a) the datum case without control devices, b) the Forwards wedges, c) the joined Counter-rotating vanes and c) the Counter-rotating vanes spaced apart by 1h, all of which were of 10 mm height. All the devices reduce the length of the separation region but the split vanes are the most effective in this respect. This result is consistent with the observation that the decay of the vortices downstream of the split vanes is much lower than that of the Forwards wedge and the joined vanes.

Contours of constant streamwise velocity are shown in Figure 10 in various cross-flow planes for the Forwards wedge and the Counter-rotating vanes that are spaced apart by 1h. The latter devices clearly induce much larger disturbances in the flow separation region near the trailing edge of the bump, indicating why these devices are more effective than the wedges. Although no picture is included here, it can be stated that the results for the joined Counter-rotating vanes resemble more closely the flowfield of the wedges than that of the split vane device.

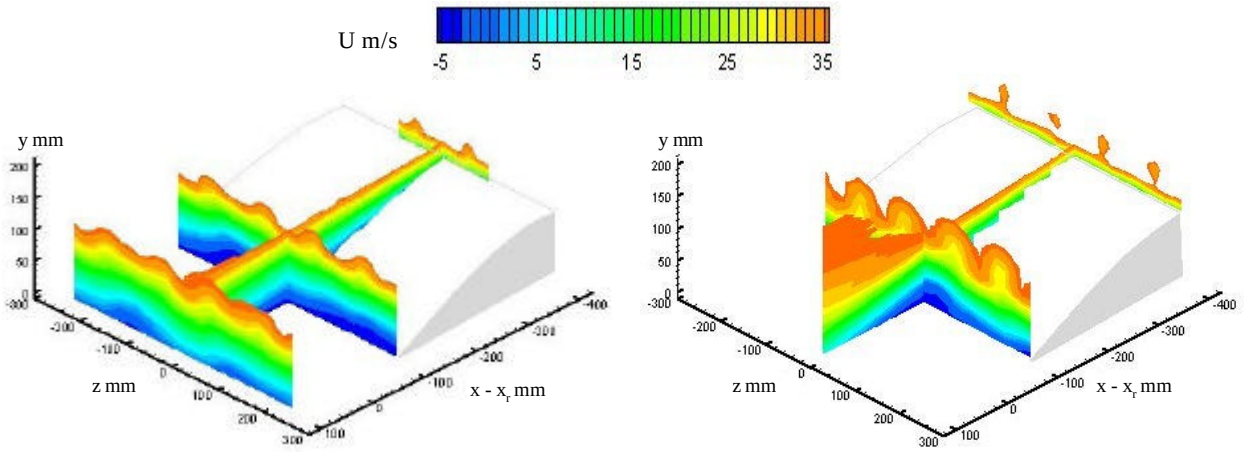

a) Forwards wedges

b) Counter-rotating vanes spaced apart 1h

Figure 10 Isometric views showing contours of constant streamwise velocity in cross-flow planes.

7. Conclusions

A detailed study of the flow downstream of various of types of Sub Boundary-layer Vortex Generators (SBVGs) has enabled a number of conclusions to be reached:

a) Single devices in zero streamwise pressure gradient

1) Correlations for the vortex strength just downstream of several different types of SBVG against device Reynolds number have been developed using the concept of an effective device height. These correlations may be used for prediction purposes.
2) The streamwise decay of vortex strength of Counter-rotating vane devices that are spaced apart by at least 1 device height is an order of magnitude lower on a logarithmic basis than that of joined Counter-rotating vanes and wedges. The vortices induced by single rotation vanes decay downstream of the device in way that is similar to that of the counter-rotating devices with spacing between the vortices.

b) Counter-rotating vane device in an adverse streamwise pressure gradient

1) The non-dimensional vortex strength is affected by pressure gradient such that the effective height of the device is reduced. However, when this effective height is used to redefine the non-dimensional vortex strength and Reynolds number the data are in reasonable accord with the correlation for zero pressure gradient flows.
2) The decay in vortex strength is similar to that in zero streamwise pressure gradient.
3) The vortex paths in the cross-flow plane show a much more pronounced tendency for outward displacement and asymmetry than is apparent in the corresponding zero pressure gradient case.

c) Pulsed jet vortex generators in a zero streamwise pressure gradient.

1) The primary vortex appears to be a function of jet velocity ratio.
2) Pulsing is an effective way to produce persistent vortices while greatly reducing the mass flow required by steady jets of a similar geometry.

d) Control of flow separation

1) Of the three types of SBVG array studied, Forwards wedges, joined Counter-rotating vanes and Counter-rotating vanes spaced apart by 1 device height, the last was the most effective in reducing the extent of the flow separation. This observation is consistent with the result of the study of vortex decay in zero pressure gradient which showed that the spaced devices gave the lowest vortex decay rate of the three types of device.

References

1 RAE TR 79040 (East, Sawyer and Nash)

2. Tilman C P, Langan K J, Betterton J G, Wilson M J, “Characterisation of pulsed vortex generator jets for active flow control,” RTO/AVT Symposium, Germany, 8-11 May 2000

3 P R Ashill, J L Fulker, K C Hackett, “Research at DERA on Sub Boundary Layer Vortex Generators” AIAA 2000-tbc.

4. Lin J C, “Control of turbulent boundary-layer separation using micro-vortex generators,” AIAA 99-3404, June 1999.

5 J C Lin, R J McGhee and W O Valarezo, “Separation control on high lift airfoils via micro-vortex generators”, Journal of Aircraft, Vol. 31, No. 6, Nov. – Dec. 1994

6. Broardly J I, “the control of trailing edge separation on highly swept wings using vortex generators,” Total technology PhD, College of Aeronautics, Cranfield, UK. October 1998

7 L F East, P D Smith and P J Merryman, “Prediction of the development of separated turbulent boundary layers by the lag entrainment method”, RAE TR 77046, 1977.

8 “Vortex generators for control of shock-induced separation. Part 1: introduction and aerodynamics”, ESDU Transonic data memorandum 93024, Dec, 1993.

9. Broardly J I, Garry KP, “Effectiveness of vortex generator position and orientation on highly swept wings,” AIAA 97-2319, June 1997.

10. Ashill P R, Riddle G L, Stanley M J, “Separation control on highly-swept wings with fixed or variable camber,” Aeronautical Journal Royal Aeronautical Society, Vol 99, No 988, October 1995.

11. Ashill P R, Fulker J L, “A review of flow control research at DERA,” Proc. Of IUTAM Symposium FLOWCON (1998).

12. Betts C J, Ashill P R, Hackett K C, “Fundamental investigations of the flow about devices suitable for use in flow control,” Proc. Of IUTAM Symposium FLOWCON (1998).

13. Wheeler G O, “Means of maintaining attached flow of a flow medium,” US patent No 4455045, 1984

14. Wheeler G O, “Low drag vortex generators,” US Patent No 5058837, 1991

15 J P Jones, “The calculation of the paths of vortices from a system of vortex generators, and a comparison with experiment”, ARC 361, 1955.

16 H H Pearcey, “Shock-induced separation and its prevention by design and boundary-layer control”, In “Boundary Layer and Flow Control, its Principles and Application”, Vol. 2, Edited by G V Lachmann, Pergamon Press, Oxford, 1961.

17 B J Wendt, J Greber and W R Hingst, “The structure and development of streamwise vortex arrays embedded in a turbulent boundary layer”, NASA Tech Memo 105211, 1991.

18 W J Duncan, A S Thom and A D Young, “The mechanics of fluids”, Edward Arnold, London, 1960.